This document is a preprint of: A. Nimr, M. Chafii and G. Fettweis, "Low-complexity Transceiver for GFDM systems with Partially Allocated Subcarriers," in Proceedings of IEEE Wireless Communications and Networking Conference (WCNC 2019), Marrakech, Morocco, Apr 2019. DOI:10.1109/WCNC.2019.8886058

Low-Complexity Transceiver for GFDM systems with Partially Allocated Subcarriers

Ahmad Nimr*, Marwa Chafii†, Gerhard Fettweis*
*Vodafone Chair Mobile Communication Systems, Technische Universität Dresden, Germany
†ENSEA, ETIS, Université Paris-Seine, CNRS, France
ahmad.nimr@ifn.et.tu-dresden.de, marwa.chafii@ensea.fr, gerhard.fettweis@tu-dresden.de

***Abstract*—The conventional receiver designs of generalized frequency division multiplexing (GFDM) system assume full subcarrier allocation. In this case, the optimal linear receivers can be implemented with low-complexity channel equalization followed by zero-forcing (ZF) demodulation. In some use cases, e.g. multiuser, only a subset of the subcarriers is active for data transmission. Therefore, the optimal receiver design needs to consider the effective joint channel and modulation matrix, which complicates the practical implementation. To maintain low-complexity realization in these cases, full allocation can still be assumed, however, the performance loss is remarkable. In this paper, we propose an efficient transceiver design for non-fully allocated GFDM system. In the proposed approach, the frequency-domain (FD) sparsity of GFDM is exploited to represent the transmitted signal by means of an effective small-size GFDM model with one non-active subcarrier. Therefore, the assumption of full allocation becomes more realistic. Moreover, the received signal can be further reformulated with fully allocated system, but at the cost of altering the effective channel gains. The proposed design significantly reduces the computation cost of the practical GFDM receiver, whereas the performance still approaches the counterpart optimal linear receiver.**

***Index Terms*—GFDM, multiuser, ZF, LMMSE, low-complexity**

I. Introduction

The flexibility of generalized frequency division multiplexing (GFDM) [1] is an attractive feature that can be exploited to design and process waveforms for different use cases. Moreover, the well-defined structure of GFDM enables a feasible real-time hardware implementation of the GFDM modem [2]. With additional processing on top, such as filtering, windowing and precoding, a flexible waveform generator is developed in [3]. For practical implementation, GFDM linear receivers can be decoupled into channel equalization (CEq) followed by demodulation. However, the design of an optimal receiver needs to consider the large scale joint channel and modulation matrix [4]. Under the assumption of full allocation, the optimal zero-forcing (ZF) receiver is obviously equivalent to GFDM receiver with ZF-CEq and ZF demodulation. On the other hand, the optimal linear minimum mean squared error (LMMSE) receiver can be implemented with LMMSE-CEq and ZF demodulation. When the modulation matrix is orthogonal, the LMMSE equalization is simple [5]. Moreover, a low complexity equalization can be achieved in the non-orthogonal case, by exploiting the block circularity of the joint matrix [6]. On the contrary, the computation of the optimal linear receivers becomes challenging when non-orthogonality *and* partial allocation are used. Although full allocation can still be assumed in this case, the performance degrades with the increase of the number of non-allocated subcarriers. In addition, using the conventional subcarrier allocation scheme of generalized frequency division multiple access (GFDMA) [7] implies unnecessary computations. In particular, asynchronous multiple access [8] requires a well-localized frequency-domain (FD) sparse GFDM filter [9]. Accordingly, the computation cost can be reduced by exploiting the FD sparsity not only at the transmitter [10], but also at the receiver.

In this paper, we focus on non-orthogonal modulation with non-full allocation, which arises in multiuser scenarios. Here, we consider the GFDMA scheme, where each user is assigned a small set of the subcarriers. Based on the FD sparsity of the filter, an effective signal model is proposed. In this model, the FD samples are generated using a *small-size* GFDM modulator corresponding to the number of allocated subcarriers in addition to one non-active subcarrier. Afterwards, the samples are allocated to the corresponding subcarriers. Compared with the conventional GFDMA, the resource allocation is performed on the FD block instead of the data symbol matrix. Similarly, the deallocation is performed on the received block to extract the effective signal, which can be expressed using the *small-size* model of the transmitter. Thus, the CEq needs to only consider the effective channel coefficients, and the assumption of full allocation is more realistic. Moreover, by means of pre-equalization and superposition of the edge subcarriers, the *effective* signal can be reformulated in form of a *small-size* fully allocated GFDM model at the receiver. However, this causes a decrease of the signal-to-noise ratio (SNR) at some samples and slightly affects the bit error rate (BER) performance. In addition to a significant complexity reduction, the numerical simulations show that the proposed linear receivers approach the BER performance of the related optimal receivers.

The remainder of the paper is organized as follows: Section II introduces an overview of FD-GFDM modem. Section III is dedicated for the design of GFDM linear receivers. In Section IV, we present the effective signal model and show its application for GFDMA in Section V. Section VI provides numerical results. Finally, Section VII concludes the paper.

This work has received funding from the European Union's Horizon 2020 research and innovation program under grant agreements No 777137 (5GRANGE project) and No 732174 (ORCA Project [https://www.orca-project.eu/]).

© 2019 IEEE. Personal use of this material is permitted. Permission from IEEE must be obtained for all other uses, in any current or future media, including reprinting/republishing this material for advertising or promotional purposes, creating new collective works, for resale or redistribution to servers or lists, or reuse of any copyrighted component of this work in other works.

This document is a preprint of: A. Nimr, M. Chafii and G. Fettweis, "Low-complexity Transceiver for GFDM systems with Partially Allocated Subcarriers," in Proceedings of IEEE Wireless Communications and Networking Conference (WCNC 2019), Marrakech, Morocco, Apr 2019. DOI:10.1109/WCNC.2019.8886058

II. FD-GFDM MODEM

Consider a GFDM system [1] with K subcarriers, M subsymbols, $N = MK$, and modulator pulse defined by the vector $\boldsymbol{g} \in \mathbb{C}^{N\times 1}$, $g[n] = [\boldsymbol{g}]_{(n)}$. Let $\boldsymbol{D} \in \mathbb{C}^{K\times M}$ be the data matrix, where $[\boldsymbol{D}]_{(k,m)} = d_{k,m}$ is the data symbol transmitted on the k-th subcarrier and m-th subsymbol. The time-domain (TD)-GFDM block $\boldsymbol{x} \in \mathbb{C}^{N\times 1}$ is given by

$$[\boldsymbol{x}]_{(n)} = \sum_{k=0}^{K-1}\sum_{m=0}^{M-1} [\boldsymbol{D}]_{(k,m)}\, g[< n - mK >_N] e^{j2\pi \frac{kn}{K}}. \quad (1)$$

The FD block is defined by $\tilde{\boldsymbol{x}} = \frac{1}{\sqrt{N}}\boldsymbol{F}_N\boldsymbol{x}$, where $\boldsymbol{F}_N$ is the N-discrete Fourier transform (DFT) matrix, $[\boldsymbol{F}_N]_{(n,n)} = e^{-j2\pi\frac{nm}{N}}$, and $< . >_N$ is the modulo-N operator. Thereby,

$$[\tilde{\boldsymbol{x}}]_{(n)} = \sum_{k=0}^{K-1}\sum_{m=0}^{M-1} [\boldsymbol{D}]_{(k,m)}\, \tilde{g}[< n - kM >_N] e^{-j2\pi \frac{mn}{M}}. \quad (2)$$

Here, $\tilde{g}[n]$ is the FD modulator pulse, $\tilde{g} = \frac{1}{\sqrt{N}}\boldsymbol{F}_N\boldsymbol{g}$.

A. Full matrix representation

The equivalent matrix model can be expressed as $\tilde{\boldsymbol{x}} = \tilde{\boldsymbol{A}}\boldsymbol{d}$, $\boldsymbol{d} = \mathrm{vec}\{\boldsymbol{D}\}$, where $\tilde{\boldsymbol{A}} \in \mathbb{C}^{N\times N}$ is defined by

$$\left[\tilde{\boldsymbol{A}}\right]_{(n,k+mK)} = \tilde{g}[< n - kM >_N] e^{-j2\pi\frac{mn}{M}}. \quad (3)$$

Any matrix satisfies (3) is referred as FD-GFDM matrix. The FD-GFDM demodulator uses an FD-GFDM matrix $\tilde{\boldsymbol{B}}$, which is generated from a demodulator pulse $\tilde{\gamma}[n]$ as in (3), such that $\hat{\boldsymbol{d}} = \tilde{\boldsymbol{B}}^H\tilde{\boldsymbol{y}}_{\text{eq}}$, where $\tilde{\boldsymbol{y}}_{\text{eq}}$ is the equalized block. Therefore,

$$\hat{d}_{k,m} = \sum_{n=0}^{N-1} [\tilde{\boldsymbol{y}}_{\text{eq}}]_{(n)}\, \tilde{\gamma}^*[< n - mK >_N] e^{j2\pi\frac{nm}{M}}. \quad (4)$$

B. Effective matrix model

In general, the data matrix $\boldsymbol{D}$ is not necessary fully loaded with data symbols. Let $\mathcal{K}_u$, $\mathcal{M}_u$ be the sets of allocated subcarriers and subsymbols, respectively. Accordingly, we define the set of active resources $\mathcal{N}_u = \{n = k+mK,\ (k,m) \in \mathcal{K}_u \times \mathcal{M}_u\}$ with $N_u = |\mathcal{N}_u|$ elements. A data vector $\boldsymbol{d}^{(u)} \in \mathbb{C}^{N_u\times 1}$ is mapped to $\boldsymbol{d}$ using a mapping matrix $\boldsymbol{\Pi}_u \in \mathbb{C}^{N\times N_u}$, such that $\boldsymbol{d} = \boldsymbol{\Pi}_u\boldsymbol{d}^{(u)}$. Therefore,

$$\tilde{\boldsymbol{x}} = \tilde{\boldsymbol{A}}\boldsymbol{\Pi}_u\boldsymbol{d}^{(u)} = \tilde{\boldsymbol{A}}_u\boldsymbol{d}^{(u)},\ \tilde{\boldsymbol{A}}_u = \left[\tilde{\boldsymbol{A}}\right]_{(:,\mathcal{N}_u)}. \quad (5)$$

Here, $\tilde{\boldsymbol{A}}_u$ is defined by selecting the columns of $\tilde{\boldsymbol{A}}$ w.r.t. to the active resource indexes. In this case, the conventional demodulator, first demodulates the received block and then extracts the allocated data. This is equivalent to the operation $\hat{\boldsymbol{d}}^{(u)} = \tilde{\boldsymbol{B}}_u^H\tilde{\boldsymbol{y}}_{\text{eq}},\ \tilde{\boldsymbol{B}}_u = \tilde{\boldsymbol{B}}\boldsymbol{\Pi}_u$.

C. Alternative representation

An alternative representation allows the derivation of low-complexity GFDM modem implementation architectures [11]. From a vector $\boldsymbol{a} \in \mathbb{C}^{PQ\times 1}$, we construct a matrix of size $\boldsymbol{V}_{Q,P}^{(\boldsymbol{a})} \in \mathbb{C}^{Q\times P}$ by unvectorizing in rows, such that

$$\boldsymbol{V}_{Q,P}^{(\boldsymbol{a})} = \mathrm{unvec}_{P\times Q}\{\boldsymbol{a}\}^T \Leftrightarrow \left[\boldsymbol{V}_{Q,P}^{(\boldsymbol{a})}\right]_{(q,p)} = [\boldsymbol{a}]_{(p+qP)}. \quad (6)$$

Using this notation, the FD block (2) can be expressed as [12]

$$\left[\boldsymbol{V}_{K,M}^{(\tilde{\boldsymbol{x}})}\right]_{(q,p)} = \sum_{k=0}^{K-1}\left[\boldsymbol{V}_{K,M}^{(\tilde{\boldsymbol{g}})}\right]_{(<q-k>_K,p)} [\boldsymbol{D}\boldsymbol{F}_M]_{(k,p)}, \quad (7)$$

which defines a circular convolution between the p-th column of $\boldsymbol{V}_{K,M}^{(\tilde{\boldsymbol{g}})}$ and the p-th column of $\boldsymbol{D}\boldsymbol{F}_M$. This can be represented by means of K-IDFT in the form

$$\boldsymbol{V}_{K,M}^{(\tilde{\boldsymbol{x}})} = \boldsymbol{F}_K\left(\boldsymbol{W}_{\text{tx}} \odot \left[\frac{1}{K}\boldsymbol{F}_K^H\boldsymbol{D}\boldsymbol{F}_M\right]\right),\ \boldsymbol{W}_{\text{tx}} = \boldsymbol{F}_K^H\boldsymbol{V}_{K,M}^{(\tilde{\boldsymbol{g}})}. \quad (8)$$

Here, $\odot$ is the element-wise product, $\boldsymbol{W}_{\text{tx}}$ is the modulator window. The demodulator uses a window $\boldsymbol{W}_{\text{rx}}$, e.g. ZF, where $[\boldsymbol{W}_{\text{rx}}]_{(k,m)} = 1/[\boldsymbol{W}_{\text{tx}}]_{(k,m)}$, such that

$$\hat{\boldsymbol{D}} = \frac{1}{M}\boldsymbol{F}_K\left(\boldsymbol{W}_{\text{rx}} \odot \left[\frac{1}{K}\boldsymbol{F}_K^H\boldsymbol{V}_{K,M}^{(\tilde{\boldsymbol{y}}_{\text{eq}})}\right]\right)\boldsymbol{F}_M^H. \quad (9)$$

III. GFDM LINEAR RECEIVERS IN FADING CHANNEL

Assuming a cyclic prefix (CP), longer than the channel delay spread, appended to the beginning of each GFDM block, the FD received block can be expressed as

$$\tilde{\boldsymbol{y}} = \boldsymbol{\Lambda}^{(\tilde{h})}\tilde{\boldsymbol{x}} + \tilde{\boldsymbol{v}},\ \tilde{\boldsymbol{x}} = \tilde{\boldsymbol{A}}_u\boldsymbol{d}^{(u)}, \quad (10)$$

where $\boldsymbol{\Lambda}^{(\tilde{h})} = \mathrm{diag}\{N\text{-DFT}\{h\}\}$ is the equivalent diagonal channel matrix, and $\tilde{\boldsymbol{v}}$ is additive white Gaussian noise (AWGN) with a variance N_0. We use the following definition:

Definition 1. *A GFDM-based receiver decouples the detection process into CEq with $\boldsymbol{H}_{eq} \in \mathbb{C}^{N\times N}$ followed by demodulation with GFDM matrix $\tilde{\boldsymbol{B}}$.*

A. LMMSE receiver

The LMMSE-CEq can be derived considering the signal model $\tilde{\boldsymbol{y}} = \boldsymbol{\Lambda}^{(\tilde{h})}\tilde{\boldsymbol{x}} + \tilde{\boldsymbol{v}}$. Assuming uncorrelated data, i.e. $\mathrm{E}\left[\boldsymbol{d}^{(\mathrm{u})}\boldsymbol{d}^{(\mathrm{u})H}\right] = E_s\boldsymbol{I}_{N_u}$, where E_s is the average symbol power, $\boldsymbol{R}_{\tilde{x}} = \mathrm{E}\left[\tilde{\boldsymbol{x}}\tilde{\boldsymbol{x}}^H\right] = E_s\tilde{\boldsymbol{A}}_u\tilde{\boldsymbol{A}}_u^H$, the CEq matrix is given by

$$\boldsymbol{H}_{\text{LMMSE}}^H = \tilde{\boldsymbol{A}}_u\tilde{\boldsymbol{A}}_u^H\boldsymbol{\Lambda}^{(\tilde{h})H}\left(\boldsymbol{\Lambda}^{(\tilde{h})}\tilde{\boldsymbol{A}}_u\tilde{\boldsymbol{A}}_u^H\boldsymbol{\Lambda}^{(\tilde{h})H} + \tfrac{N_0}{E_s}\boldsymbol{I}_N\right)^{-1}. \quad (11)$$

On the other hand, the joint LMMSE considers the combined channel and modulation matrix, $\tilde{\boldsymbol{y}} = [\boldsymbol{\Lambda}^{(\tilde{h})}\tilde{\boldsymbol{A}}_u]\boldsymbol{d}^{(u)} + \tilde{\boldsymbol{v}}$. Thus,

$$\begin{aligned}\boldsymbol{W}_{\text{MMSE}}^H &= \tilde{\boldsymbol{A}}_u^H\boldsymbol{\Lambda}^{(\tilde{h})H}\left(\boldsymbol{\Lambda}^{(\tilde{h})}\tilde{\boldsymbol{A}}_u\tilde{\boldsymbol{A}}_u^H\boldsymbol{\Lambda}^{(\tilde{h})H} + \tfrac{N_0}{E_s}\boldsymbol{I}_N\right)^{-1}\\ &= \boldsymbol{\Pi}_u^T\tilde{\boldsymbol{A}}^{-1}\boldsymbol{H}_{\text{LMMSE}}^H.\end{aligned} \quad (12)$$

Note that if $\tilde{\boldsymbol{A}}$ is non-singular, then $\tilde{\boldsymbol{A}}^{-1H}$ is a valid FD-GFDM matrix [13]. Based on that, the optimal LMMSE receiver can be performed by means of GFDM receiver, which consists of LMMSE-CEq followed by ZF-demodulation and deallocation. However, the computation of $\boldsymbol{H}_{\text{LMMSE}}^H$ generally requires the computation of the inverse of $N\times N$ matrix. Alternatively, the joint LMMSE can also be computed as

$$\boldsymbol{W}_{\text{MMSE}}^H = \left(\tilde{\boldsymbol{A}}_u^H\boldsymbol{\Lambda}^{(\tilde{h})H}\boldsymbol{\Lambda}^{(\tilde{h})}\tilde{\boldsymbol{A}}_u + \frac{N_0}{E_s}\boldsymbol{I}_{N_u}\right)^{-1}\tilde{\boldsymbol{A}}_u^H\boldsymbol{\Lambda}^{(\tilde{h})H}. \quad (13)$$

This can be performed with matched filter (MF)-GFDM receiver using MF-CEq followed by MF-demodulation and deallocation, i.e. $\boldsymbol{\Pi}_u^T\tilde{\boldsymbol{A}}^H\boldsymbol{\Lambda}^{(\tilde{h})H}$. The remaining part of the receiver

© 2019 IEEE. Personal use of this material is permitted. Permission from IEEE must be obtained for all other uses, in any current or future media, including reprinting/republishing this material for advertising or promotional purposes, creating new collective works, for resale or redistribution to servers or lists, or reuse of any copyrighted component of this work in other works.

This document is a preprint of: A. Nimr, M. Chafii and G. Fettweis, "Low-complexity Transceiver for GFDM systems with Partially Allocated Subcarriers," in Proceedings of IEEE Wireless Communications and Networking Conference (WCNC 2019), Marrakech, Morocco, Apr 2019. DOI:10.1109/WCNC.2019.8886058

can be seen as an interference cancellation, which requires the inversion of a matrix of size $N_u \times N_u$. Nevertheless, the implementation of both models is practically complicated. However, in the case of full allocation, i.e. $\tilde{\boldsymbol{A}}_u = \tilde{\boldsymbol{A}}$, we get

$$\boldsymbol{H}_{\text{eq}}^{H} = \boldsymbol{\Lambda}^{(\tilde{h})H} \left(\boldsymbol{\Lambda}^{(\tilde{h})H} \boldsymbol{\Lambda}^{(\tilde{h})} + \frac{N_0}{E_s} \left[\tilde{\boldsymbol{A}} \tilde{\boldsymbol{A}}^{H} \right]^{-1} \right)^{-1}, \tag{14}$$

which can be more efficiently computed [6].

B. ZF receiver

The joint ZF receiver can be expressed as

$$\boldsymbol{W}_{\text{ZF}}^{H} = \left(\tilde{\boldsymbol{A}}_u^{H} \boldsymbol{\Lambda}^{(\tilde{h})H} \boldsymbol{\Lambda}^{(\tilde{h})} \tilde{\boldsymbol{A}}_u \right)^{-1} \tilde{\boldsymbol{A}}_u^{H} \boldsymbol{\Lambda}^{(\tilde{h})H}. \tag{15}$$

This receiver cannot be decoupled into ZF-CEq and ZF-demodulator unless full allocation ($\tilde{\boldsymbol{A}}_u = \tilde{\boldsymbol{A}}$) is used. However, a practical ZF-GFDM receiver performs a simple ZF-CEq, i.e. $\boldsymbol{H}_{\text{ZF}}^{H} = \boldsymbol{\Lambda}^{(\tilde{h})-1}$ followed by ZF-demodulation and deallocation. In the case of full allocation, the optimal ZF and ZF-GFDM are equivalent. Otherwise, the simplicity of ZF-GFDM is at the cost of performance loss.

C. LMMSE equalization under full subcarrier allocation

The received block in (10) can be reformulated using (6) as

$$\boldsymbol{V}_{K,M}^{(\tilde{\boldsymbol{y}})} = \boldsymbol{V}_{K,M}^{(\tilde{\boldsymbol{h}})} \odot \boldsymbol{V}_{K,M}^{(\tilde{\boldsymbol{x}})} + \boldsymbol{V}_{K,M}^{(\tilde{\boldsymbol{v}})}. \tag{16}$$

We define the shorthand notations $\tilde{\boldsymbol{d}}_m = [\boldsymbol{D}\boldsymbol{F}_M]_{(:,m)}$, $\tilde{\boldsymbol{x}}_m = \left[\boldsymbol{V}_{K,M}^{(\tilde{\boldsymbol{x}})}\right]_{(:,m)}$, $\boldsymbol{\Lambda}_m^{(\tilde{h})} = \text{diag}\left\{\tilde{\boldsymbol{h}}_m\right\}$ and $\boldsymbol{\Lambda}_m^{(\text{tx})} = \text{diag}\left\{[\boldsymbol{W}_{\text{tx}}]_{(:,m)}\right\}$. By taking the m-th column of (16) and using (8) we get

$$\tilde{\boldsymbol{y}}_m = \boldsymbol{\Lambda}_m^{(\tilde{h})} \tilde{\boldsymbol{A}}_m \tilde{\boldsymbol{d}}_m + \tilde{\boldsymbol{v}}_m, \;\; \tilde{\boldsymbol{A}}_m = \frac{1}{K} \boldsymbol{F}_K \boldsymbol{\Lambda}_m^{(\text{tx})} \boldsymbol{F}_K^{H}. \tag{17}$$

Consider full subcarrier allocation, $\mathcal{K}_u = \{0, \cdots, K-1\}$, $0 < M_u = |\mathcal{M}_u| \leq M$, and uncorrelated data symbols. Thus, $\text{E}\left[\tilde{\boldsymbol{d}}_m \tilde{\boldsymbol{d}}_p^{H}\right] = E_s [\boldsymbol{\Omega}]_{(p,m)} \boldsymbol{I}_K$, $\boldsymbol{\Omega} = [\boldsymbol{F}_M]_{(:,\mathcal{M}_u)} \left[\boldsymbol{F}_M^{H}\right]_{(\mathcal{M}_u,:)}$. If all subsymbols are allocated, then $\boldsymbol{\Omega} = M\boldsymbol{I}_K$. Therefore, (17) represents M uncorrelated streams. In some use cases, the first subsymbol is turned off, e.g. to achieve low out-of-band (OOB) [14], i.e. $M_u = M-1$. In this case, $[\boldsymbol{\Omega}]_{(p,m)} = -1, m \neq p$, and $[\boldsymbol{\Omega}]_{(m,m)} = M-1$. Thereby, the M substreams can be assumed uncorrelated when M is large. Under this assumption, the LMMSE-CEq can be computed using the substreams, $\tilde{\boldsymbol{y}}_m = \boldsymbol{\Lambda}_m^{(\tilde{h})} \tilde{\boldsymbol{x}}_m + \tilde{\boldsymbol{v}}_m$, $\tilde{\boldsymbol{x}}_m = \tilde{\boldsymbol{A}}_m \tilde{\boldsymbol{d}}_m$, with $\tilde{\boldsymbol{H}}_{m,\text{eq}}^{H}$ is given by

$$\tilde{\boldsymbol{H}}_{m,\text{eq}}^{H} = \left({\boldsymbol{\Lambda}_m^{(\tilde{h})}}^{H} \boldsymbol{\Lambda}_m^{(\tilde{h})} + N_0 \boldsymbol{R}_m^{-1} \right)^{-1} {\boldsymbol{\Lambda}_m^{(\tilde{h})}}^{H}, \tag{18}$$

where $\boldsymbol{R}_m = \text{E}\left[\tilde{\boldsymbol{x}}_m \tilde{\boldsymbol{x}}_m^{H}\right] = \frac{M_u E_s}{K} \boldsymbol{F}_K \boldsymbol{\Lambda}_m^{(\text{tx})} \boldsymbol{\Lambda}_m^{(\text{tx})H} \boldsymbol{F}_K^{H}$. If the elements of $\boldsymbol{\Lambda}_m^{(\text{tx})}$ are of equal amplitude, then $\boldsymbol{R}_m$ is diagonal and thus $\tilde{\boldsymbol{H}}_{m,\text{eq}}^{H}$ is diagonal. For instance, in conventional GFDM with two-subcarrier overlap, depending on the roll-off factor, there are several indexes where $\boldsymbol{\Lambda}_m^{(\text{tx})}$ satisfies this condition [9]. Otherwise, a diagonal approximation is obtained by ignoring the correlation between the elements of $\tilde{\boldsymbol{x}}_m$, i.e. $\boldsymbol{R}_m \approx \frac{M_u E_s}{K} P_m^{(\text{tx})} \boldsymbol{I}_K$, where $P_m^{(\text{tx})} = \text{trace}\left\{\boldsymbol{\Lambda}_m^{(\text{tx})} \boldsymbol{\Lambda}_m^{(\text{tx})H}\right\}$. Thus,

$$\tilde{\boldsymbol{\Lambda}}_{m,\text{eq}}^{H} = \left({\boldsymbol{\Lambda}_m^{(\tilde{h})}}^{H} \boldsymbol{\Lambda}_m^{(\tilde{h})} + \frac{N_0 K}{E_s M_u P_m^{(\text{tx})}} \right)^{-1} {\boldsymbol{\Lambda}_m^{(\tilde{h})}}^{H}, \tag{19}$$

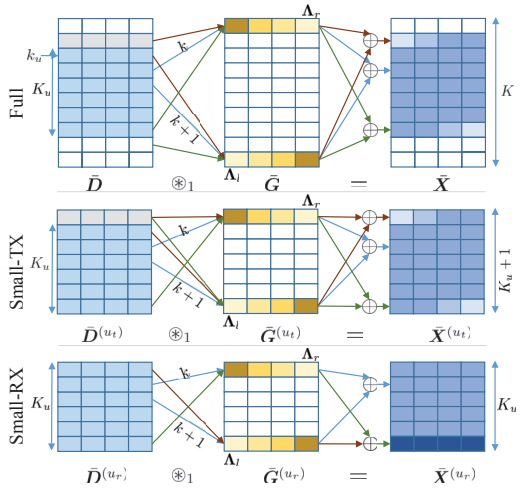

Fig. 1: Conventional GFDM effective representation.

IV. Conventional GFDM Effective Representation

In conventional GFDM, the prototype pulse shape is designed with maximum two-subcarrier overlap [9]. Without lost of generality, let $\tilde{g}[< n >_N] = 0$, $n \notin \{-M, \cdots, M-1\}$. Accordingly, $\boldsymbol{V}_{K,M}^{(\tilde{\boldsymbol{g}})}$ contains only two non-zero rows at the indexes $k = 0$ and $k = K-1$. For notation simplicity, let $\bar{\boldsymbol{D}} = \boldsymbol{D}\boldsymbol{F}_M$, $\bar{\boldsymbol{X}} = \boldsymbol{V}_{K,M}^{(\tilde{\boldsymbol{x}})}$, $\bar{\boldsymbol{G}} = \boldsymbol{V}_{K,M}^{(\tilde{\boldsymbol{g}})}$, $\bar{\boldsymbol{d}}_k = \left[\bar{\boldsymbol{D}}^{T}\right]_{(:,<k>_K)}$, $\bar{\boldsymbol{x}}_k = \left[\bar{\boldsymbol{X}}^{T}\right]_{(:,<k>_K)}$, $\boldsymbol{\Lambda}_r = \text{diag}\left\{[\bar{\boldsymbol{G}}]_{(0,:)}\right\}$, $\boldsymbol{\Lambda}_l = \text{diag}\left\{[\bar{\boldsymbol{G}}]_{(K-1,:)}\right\}$.With that, the convolution (7) can be expressed as

$$\begin{aligned}[\bar{\boldsymbol{X}}]_{(q,p)} &= \sum_{k=0}^{K-1} [\bar{\boldsymbol{G}}]_{(k,p)} [\bar{\boldsymbol{D}}]_{(<q-k>_K,p)} \\ &= [\bar{\boldsymbol{G}}]_{(0,p)} [\bar{\boldsymbol{D}}]_{(q,p)} + [\bar{\boldsymbol{G}}]_{(K-1,p)} [\bar{\boldsymbol{D}}]_{(<q+1>_K,p)}.\end{aligned}$$

Therefore,

$$\bar{\boldsymbol{x}}_k = \boldsymbol{\Lambda}_r \bar{\boldsymbol{d}}_k + \boldsymbol{\Lambda}_l \bar{\boldsymbol{d}}_{k+1}. \tag{20}$$

As a result, the k-th subcarrier contributes to frequency samples in $\bar{\boldsymbol{x}}_k$ and $\bar{\boldsymbol{x}}_{k-1}$, as depicted in Fig. 1. Moreover, the conventional FD-GFDM with K subcarriers can be written as

$$\bar{\boldsymbol{X}} = \bar{\boldsymbol{D}} \boldsymbol{\Lambda}_r + \boldsymbol{P}_1^{(K)} \bar{\boldsymbol{D}} \boldsymbol{\Lambda}_l, \tag{21}$$

where $\boldsymbol{P}_1^{(K)}$ is $K \times K$ circular shift matrix with a shift of 1.

A. Effective small-size transmitter model

Assuming a set of contiguous $K_u < K$ active subcarriers $\mathcal{K}_u = \{< k >_K, k \in \{k_u, \cdots, k_u + K_u - 1\}$, where $-K/2 < k_u < K/2$ indicates the starting index of the active set. Thus, $\bar{\boldsymbol{d}}_k = \boldsymbol{0}_M$, $k \notin \mathcal{K}_u$. Based on (20), the non-zero rows of $\bar{\boldsymbol{X}}$ are within $\mathcal{K}_{u_t} = \{< k >_K, k \in \{k_u - 1, \cdots, k_u + K_u - 1\}$, as illustrated in Fig. 1. Accordingly, we define the matrices $\bar{\boldsymbol{X}}^{(u_t)}$, $\bar{\boldsymbol{D}}^{(u_t)} \in \mathbb{C}^{K_u+1 \times M}$, where $\bar{\boldsymbol{d}}_0^{(u_t)} = \boldsymbol{0}_M$, $\{\bar{\boldsymbol{d}}_k^{(u_t)} = \bar{\boldsymbol{d}}_{k+k_u-1}\}_{k=1}^{k=K_u}$, $\{\bar{\boldsymbol{x}}_k^{(u_t)} = \bar{\boldsymbol{x}}_{k+k_u-1}\}_{k=0}^{k=K_u}$. Therefore,

$$\bar{\boldsymbol{X}}^{(u_t)} = \bar{\boldsymbol{D}}^{(u_t)} \boldsymbol{\Lambda}_r + \boldsymbol{P}_1^{(K_u+1)} \bar{\boldsymbol{D}}^{(u_t)} \boldsymbol{\Lambda}_l. \tag{22}$$

$\bar{\boldsymbol{X}}^{(u_t)}$ represents FD-GFDM samples generated by means of small-size GFDM system with the parameters (K_u+1, M), and a transmitter pulse $\tilde{g}^{(u_t)}$ of length $N_{u_t} = (K_u+1)M$, where

© 2019 IEEE. Personal use of this material is permitted. Permission from IEEE must be obtained for all other uses, in any current or future media, including reprinting/republishing this material for advertising or promotional purposes, creating new collective works, for resale or redistribution to servers or lists, or reuse of any copyrighted component of this work in other works.

This document is a preprint of: A. Nimr, M. Chafii and G. Fettweis, "Low-complexity Transceiver for GFDM systems with Partially Allocated Subcarriers," in Proceedings of IEEE Wireless Communications and Networking Conference (WCNC 2019), Marrakech, Morocco, Apr 2019. DOI:10.1109/WCNC.2019.8886058

$\tilde{g}^{(u_t)}[< n >_{N_{u_t}}] = \tilde{g}[< n >_N], -M \leq n < M$. Therefore, the original block can be achieved via *sample allocation* $\left[\bar{\boldsymbol{X}}\right]_{(k+k_u-1,:)} = \left[\bar{\boldsymbol{X}}^{(u_t)}\right]_{(k,:)}$, and the TD block is generated as $\boldsymbol{x} = \frac{1}{\sqrt{N}}\boldsymbol{F}_N^H \text{vec}\left\{\bar{\boldsymbol{X}}^T\right\}$.

B. Effective small-size receiver model

Taking the rows of (16), we get the FD received samples

$$\bar{\boldsymbol{y}}_k = \boldsymbol{\Gamma}_k \bar{\boldsymbol{x}}_k + \bar{\boldsymbol{v}}_k,\ \boldsymbol{\Gamma}_k = \text{diag}\left\{\left[\boldsymbol{V}_{K,M}^{(\tilde{\boldsymbol{h}})}\right]_{(<k>_K,:)}\right\}. \tag{23}$$

The effective model can be achieved by sample deallocation, $\left[\bar{\boldsymbol{Y}}^{(u_t)}\right]_{(k,:)} = \left[\bar{\boldsymbol{Y}}\right]_{(k+k_u-1,:)}$, $k = 0, \cdots, K_u$, and the effective channel can be defined similarly. On the other hand, to construct a fully allocated subcarriers, we note that

$$\forall k = 0, \cdots K_u - 2,$$
$$\bar{\boldsymbol{y}}_{k+k_u-1} = \boldsymbol{\Gamma}_{k+k_u-1}\left(\boldsymbol{\Lambda}_r \bar{\boldsymbol{d}}_{k+k_u-1} + \boldsymbol{\Lambda}_l \bar{\boldsymbol{d}}_{k+k_u}\right) + \bar{\boldsymbol{v}}_{k+k_u-1}.$$

Moreover, at the edge subcarriers,

$$\begin{aligned}\bar{\boldsymbol{y}}_{k_u-1} &= \boldsymbol{\Gamma}_{k_u-1}\left(\boldsymbol{0}_M + \boldsymbol{\Lambda}_l \bar{\boldsymbol{d}}_{k_u}\right) + \bar{\boldsymbol{v}}_{k_u-1},\\ \bar{\boldsymbol{y}}_{K_u+k_u-1} &= \boldsymbol{\Gamma}_{K_u+k_u-1}\left(\boldsymbol{\Lambda}_r \bar{\boldsymbol{d}}_{K_u+k_u-1} + \boldsymbol{0}_M\right) + \bar{\boldsymbol{v}}_{K_u+k_u-1}.\end{aligned}$$

Thus, we define the matrix $\bar{\boldsymbol{D}}^{(u_r)}, \bar{\boldsymbol{Y}}^{(u_r)} \in \mathbb{C}^{K_u \times M}$ such that $\{\bar{\boldsymbol{d}}_k^{(u_r)} = \bar{\boldsymbol{d}}_{k+k_u}\}_{k=0}^{k=K_u-1}$, $\{\bar{\boldsymbol{y}}_k^{(u_r)} = \bar{\boldsymbol{y}}_{k+k_u}\}_{k=0}^{k=K_u-2}$ and $\{\boldsymbol{\Gamma}_k^{(u_r)} = \boldsymbol{\Gamma}_{k+k_u}\}_{k=0}^{k=K_u-2}$. In addition, the edge subcarriers are pre-equalized using diagonal matrices $\boldsymbol{\Psi}_l, \boldsymbol{\Psi}_r \in \mathbb{C}^{M \times M}$ and summed together to create the (K_u-1)-th subcarrier,

$$\bar{\boldsymbol{y}}_{K_u-1}^{(u_r)} = \boldsymbol{\Psi}_r \bar{\boldsymbol{y}}_{K_u+k_u-1} + \boldsymbol{\Psi}_l \bar{\boldsymbol{y}}_{k_u-1}. \tag{24}$$

To maintain the noise power,

$$|\left[\boldsymbol{\Psi}_l\right]_{(m,m)}|^2 + |\left[\boldsymbol{\Psi}_r\right]_{(m,m)}|^2 = 1. \tag{25}$$

Moreover, let $\boldsymbol{\Gamma}_{K_u-1}^{(u_r)}$ be the effective channel gain of the (K_u-1)-th subcarrier, such that

$$\boldsymbol{\Psi}_l \boldsymbol{\Gamma}_{k_u-1} \boldsymbol{\Lambda}_l = \boldsymbol{\Gamma}_{K_u-1}^{(u_r)} \boldsymbol{\Lambda}_l, \quad \boldsymbol{\Psi}_r \boldsymbol{\Gamma}_{K_u+k_u-1} \boldsymbol{\Lambda}_r = \boldsymbol{\Gamma}_{K_u-1}^{(u_r)} \boldsymbol{\Lambda}_r, \tag{26}$$

$$\text{Then, } \bar{\boldsymbol{y}}_{K_u-1}^{(u_r)} = \boldsymbol{\Gamma}_{K_u-1}^{(u_r)}\left(\boldsymbol{\Lambda}_r \bar{\boldsymbol{d}}_{K_u-1}^{(u_r)} + \boldsymbol{\Lambda}_l \bar{\boldsymbol{d}}_0^{(u_r)}\right) + \bar{\boldsymbol{v}}_{K_u-1}^{(u_r)}, \tag{27}$$

Noting that designing non-singular modulation matrix satisfies that $(\boldsymbol{\Lambda}_l + \boldsymbol{\Lambda}_r)$ is non-singular [9], then

$$\boldsymbol{\Gamma}_{K_u-1}^{(u_r)} = \left(\boldsymbol{\Psi}_l \boldsymbol{\Gamma}_{k_u-1} \boldsymbol{\Lambda}_l + \boldsymbol{\Psi}_r \boldsymbol{\Gamma}_{K_u-1}^{(u_r)} \boldsymbol{\Lambda}_r\right)\left(\boldsymbol{\Lambda}_l + \boldsymbol{\Lambda}_r\right)^{-1}. \tag{28}$$

As a result, we get an effective model with fully allocated subcarriers, which is expressed as

$$\bar{\boldsymbol{Y}}^{(u_r)} = \bar{\boldsymbol{H}}^{(u_r)} \odot \bar{\boldsymbol{X}}^{(u_r)} + \bar{\boldsymbol{V}}. \tag{29}$$

where $\bar{\boldsymbol{X}}^{(u_r)}$ is the block generated from a small-size GFDM with the parameters (K_u, M) and a pulse $\tilde{g}^{(u_r)}$ of length $N_u = K_u M$, where $\tilde{g}^{(u_r)}[< n >_{N_u}] = \tilde{g}[< n >_N], -M \leq n < M$, as illustrated in Fig. 1. Furthermore, $\bar{\boldsymbol{H}}^{(u_r)}$ is the effective channel whose rows are defined as $\left[\bar{\boldsymbol{H}}^{(u_r)}\right]_{(k,:)} = \text{diag}\left\{\boldsymbol{\Gamma}_k^{(u_r)}\right\}$.

C. Computation of pre-equalization matrices

The matrices $\boldsymbol{\Psi}_l, \boldsymbol{\Psi}_r$ are optimized to maximize the SNR of the samples of $\bar{\boldsymbol{y}}_{K_u-1}^{(u_r)}$. For notation simplicity, let $\psi_x = \left[\boldsymbol{\Psi}_x\right]_{(m,m)}$, $\lambda_x = \left[\boldsymbol{\Lambda}_x\right]_{(m,m)}, \gamma_l = \left[\boldsymbol{\Gamma}_{k_u-1}\right]_{(m,m)}, \gamma_r = \left[\boldsymbol{\Gamma}_{K_u+k_u-1}\right]_{(m,m)}, \beta = \left[\boldsymbol{\Gamma}_{K_u-1}^{(u_r)}\right]_{(m,m)}$. The SNR at the sample $\left[\bar{\boldsymbol{y}}_{K_u-1}^{(u_r)}\right]_{(m)}$ can be computed from (27) as

$$\text{SNR}_m = \frac{E_s}{N_0} \frac{|\beta|^2(|\lambda_r|^2 + |\lambda_l|^2)}{|\psi_r|^2 + |\psi_l|^2}. \tag{30}$$

From (28), $\beta = (\psi_l \gamma_l \lambda_l + \psi_r \gamma_r \lambda_r)(\lambda_r + \lambda_l)^{-1}$. Therefore, we need to maximize $\eta(\psi_r, \psi_l) = \frac{|\psi_l \gamma_l \lambda_l + \psi_r \gamma_r \lambda_r|^2}{|\psi_r|^2 + |\psi_l|^2}$ with respect to the conditions (25) and (26). When $\lambda_l \lambda_r \neq 0$,

$$\psi_r \gamma_r = \psi_l \gamma_l,\ |\psi_r|^2 + |\psi_l|^2 = 1, \tag{31}$$

the solution satisfies $|\psi_l|^2 = |\gamma_l|^2/(|\gamma_r|^2 + |\gamma_l|^2)$. Thus,

$$\psi_r = \frac{\gamma_l}{\sqrt{|\gamma_r|^2 + |\gamma_l|^2}}, \psi_l = \frac{\gamma_r}{\sqrt{|\gamma_r|^2 + |\gamma_l|^2}}. \tag{32}$$

If $\lambda_l = 0$, then $\psi_l = 0, \psi_r = 1$, and for $\lambda_r = 0$, $\psi_l = 1, \psi_r = 0$.

V. Effective GFDMA System

In conventional GFDMA, the u-th user is assigned a set of K_u contiguous subcarriers and a guard subcarrier is used to separate adjacent users to reduce the inter-user-interference. Hence, the proposed effective models can be used to reduce the complexity of the conventional GFDMA transceiver.

A. Effective transmitter

In the downlink (DL), the base station (BS) multiplexes the data from U users in the data matrix $\boldsymbol{D} \in \mathbb{C}^{K \times M}$ and applies full-size TD-GFDM modulation. In other words, the subcarrier allocation is performed at the data symbol level as seen in Fig. 2. In the effective model, the data of each user are fed to a small-size FD-GFDM with the parameters M and $(K_u + 1) \ll K$ as discussed in Section IV-A. Then, the allocation is performed on the FD samples. Afterwards, the TD block is generated by means of N-IDFT. Thus, the small-size modem is reused U times instead of using a large-size modem. This approach reduces the amount of the hardware resources required for modulator implementation [11]. Moreover, the processing power is efficiently used since the FD modulation is carried out only for the active users. However, these benefits are at the cost of increased latency, which can be compensated by increasing the processing speed. On the contrary, employing this model at the user equipment (UE) reduces the latency, where the small-size modem is executed once per block. This is faster than using full-size modem architecture. Therefore, the processing speed can be relaxed, which enables a low-cost implementation at the UE.

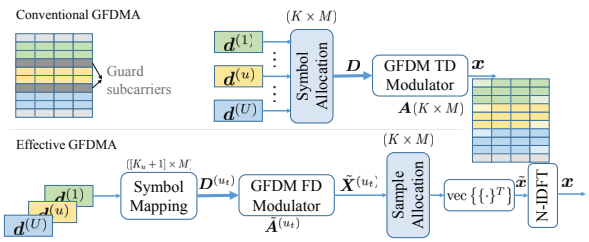

Fig. 2: Conventional and effective GFDMA transmitter.

© 2019 IEEE. Personal use of this material is permitted. Permission from IEEE must be obtained for all other uses, in any current or future media, including reprinting/republishing this material for advertising or promotional purposes, creating new collective works, for resale or redistribution to servers or lists, or reuse of any copyrighted component of this work in other works.

This document is a preprint of: A. Nimr, M. Chafii and G. Fettweis, "Low-complexity Transceiver for GFDM systems with Partially Allocated Subcarriers," in Proceedings of IEEE Wireless Communications and Networking Conference (WCNC 2019), Marrakech, Morocco, Apr 2019. DOI:10.1109/WCNC.2019.8886058

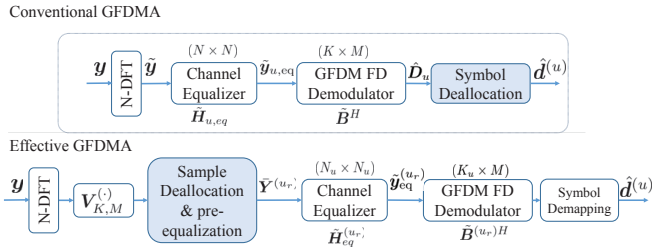

Fig. 3: Conventional and effective GFDMA receiver.

B. Effective receiver

In the conventional DL, the u-th user performs a full-size CEq followed by FD demodulation and symbol deallocation to get the estimated data $\hat{\boldsymbol{d}}^{(u)}$. The effective model as illustrated in Fig. 3 reduces the processing to the useful signal. First the effective samples are extracted via sample deallocation. Afterwards, either the full subcarrier allocation model as discussed in Section IV-B, or the small-size model with one non-active subcarrier can be used. Then, CEq is performed using the effective channel. Finally, a small-size FD demodulator is exploited. Thereby, the receiver needs to process a GFDM system of dimension $(K_u$ or $(K_u+1), M)$, $K_u \ll K$ instead of (K, M). The GFDM receiver complexity is influenced by $K \log_2 K$ [5]. Therefore, the proposed model reduces the computation cost by a factor $(K \log_2 K)/(K_u \log_2 K_u)$. In the uplink (UL), the BS performs detection per user using the small-size model instead of the full-size processing performed by the conventional GFDMA. Hence, the effective model also reduces the complexity by the factor $(K \log_2 K)/(K_u \log_2 K_u)$.

VI. Numerical Simulation

In this section, we evaluate the coded BER performance of different GFDM-based linear receivers in comparison with the optimal ones. The optimal LMMSE and ZF receivers are calculated from the effective matrix model of Section II-B using (13) and (15), respectively. The GFDM-based receivers are evaluated with different signal model at the demodulator. Accordingly, "FULL" refers to the signal model given in (10), whereas "SMALL-TX" and "SMALL-RX" denote the small-size signal models derived in Sections IV-A and IV-B, respectively. In the latter three cases, the GFDM receiver employs ZF-demodulator with a window generated from the equivalent pulse shape using (8). The receiver type is determined by the CEq method. The ZF-CEq is performed by inverting the equivalent channel. The LMMSE is computed with low-complexity using (18), whereas the diagonal approximation (19) is referred as "LMMSE-approx".

A. Simulation parameters

The data symbols are selected from 16-QAM constellation. The SNR is defined by the ratio E_b/N_0, where $E_b = E_s/4$ is the bit energy. For channel coding we employ LTE-Turbo code with rate $1/2$. All the simulations are performed using multi-tap channel model with $L = 32$ taps and exponential power-delay-profile (PDP), $P_h[l] = \frac{1}{\xi} e^{-\eta l}$, $\eta = 0.4$, $\xi = \sum_{l=0}^{L-1} e^{-\eta l}$.

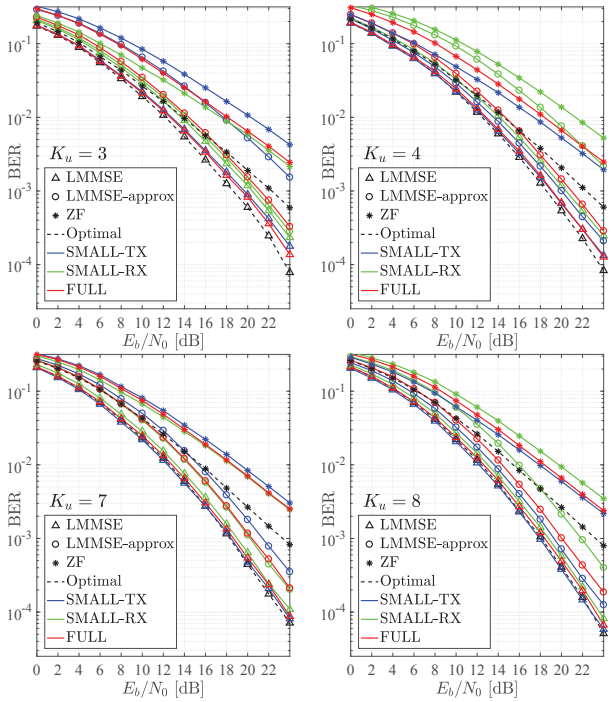

Fig. 4: BER vs E_b/N_0 for different receiver approaches.

The GFDM system is configured with $M = 16$, $K = 32$ and a periodic raised-cosine (RC) pulse shape with roll-off factor $\alpha = 0.9$ designed as in [9]. We assume a single user with K_u allocated subcarrier starting from the index $k_u = 0$.

B. Number of allocated subcarriers

In this evaluation all the subsymbols are allocated. Fig. (4) illustrates the BER performance for different number of allocated subcarriers. Considering first the ZF receiver, it can be seen that the gap between the best ZF-GFDM receiver and the optimal ZF is decreased with the increase of the number of allocated subcarriers. Moreover, the signal model of the best ZF-GFDM receiver depends on the number of subcarriers. For a even number K_u, SMALL-TX is the best one and it outperforms the FULL one. Contrarily, for odd K_u, SMALL-RX is the best. As expected, at higher SNRs and larger number of K_u all the three models achieve similar performance when using ZF-CEq. Actually, the observed performance in Fig. 4 is mainly affected by the noise-enhancement factor (NEF) of the demodulator. The NEF depends on the transmitter window and it is given by $\text{NEF} = \frac{1}{N^2} \|\boldsymbol{W}_{\text{tx}}\|_F^2 \|\boldsymbol{W}_{\text{rx}}\|_F^2$ [9]. Fig. 5 illustrates the NEF for different K_u. It shows that for odd K_u, SMALL-RX achieves lower NEF, while for even K_u SMALL-TX is the best and vice versa. On the other hand, when K_u increases, the NEF converges to a constant value, which is the NEF of the FULL model, i.e. when $K_u = 32$. The NEF also affects the performance of the receiver when LMMSE-approx is used. In this receiver, using even K_u with SMALL-TX provides BER closer to that of the optimal LMMSE. Moreover, SMALL-RX with LMMSE-approx does not provide significant gain

© 2019 IEEE. Personal use of this material is permitted. Permission from IEEE must be obtained for all other uses, in any current or future media, including reprinting/republishing this material for advertising or promotional purposes, creating new collective works, for resale or redistribution to servers or lists, or reuse of any copyrighted component of this work in other works.

This document is a preprint of: A. Nimr, M. Chafii and G. Fettweis, "Low-complexity Transceiver for GFDM systems with Partially Allocated Subcarriers," in Proceedings of IEEE Wireless Communications and Networking Conference (WCNC 2019), Marrakech, Morocco, Apr 2019. DOI:10.1109/WCNC.2019.8886058

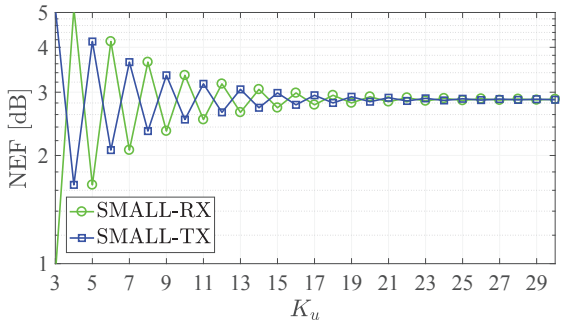

Fig. 5: NEF vs K_u, $M = 16$ and $\alpha = 0.9$.

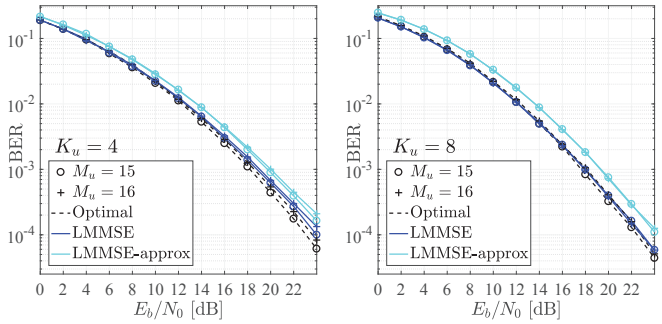

Fig. 6: BER vs E_b/N_0 using SMALL-TX.

compared with the FULL model. This is because the effective SNR at the $(K_u - 1)$-th subcarrier is reduced after pre-equalization as discussed in Section IV-C. Nevertheless, the computation cost is reduced due to the use of small-size demodulation. Furthermore, the best GFDM-based receiver with LMMSE-approx outperforms the optimal ZF, especially at higher SNR. On the other hand, LMMSE-GFDM using all the three signal models approaches the optimal LMMSE. However, using SMALL-TX is slightly better than the FULL model for even K_u and vice versa. Due to the decreased SNR at the $(K_u - 1)$-th subcarrier, SMALL-RX is slightly worse than the others in all K_u cases. In summary, SMALL-TX with LMMSE-approx and even K_u is a convenient choice, as the LMMSE equalization is very simple and the performance loss is less than 2 dB compared to the optimal LMMSE.

C. First subsymbols

In this evaluation, the first subsymbol is not allocated. The GFDM receiver employs the SMALL-TX model, and performs LMMSE or LMMSE-approx assuming full allocation. Fig. 6 compares the performance of the selected GFDM receivers with the optimal LMMSE (13). It can be seen that performing the low-complexity LMMSE with SMALL-TX still approaches the optimal LMMSE, which is more complicated for realistic implementation. Also LMMSE-approx is still very efficient and can be considered as an ideal low-complexity receiver for non-orthogonal GFDM.

VII. Conclusion

In this paper, we consider practical GFDM receivers that are implemented by means of channel equalization (CEq) and ZF demodulation. With full allocation, the optimal joint ZF and LMMSE can be realized with low-complexity GFDM counterpart receivers. Under small-size allocation and non-orthogonal modulation, low-complexity CEq can still be achieved, but the performance loss is significant. By exploiting the sparsity under partial subcarrier allocation, we represent the FD samples of the transmitted block in a form of a small-size GFDM block with only one non-active subcarrier. Accordingly, the full allocation assumption becomes more realistic. In addition, the GFDM system dimension is smaller, which reduces the computation cost. However, the BER performance is influenced by the even/odd number of allocated subcarriers, which is shown to be directly related to the NEF of the small-size GFDM system. Thus, we propose another small-size model at the receiver to achieve full subcarrier allocation at the cost of sacrificing the SNR of the edge subcarriers. As a result, the receiver can switch to the model with the lower NEF. The numerical results show that using the proposed small-size models with LMMSE-CEq approaches the optimal joint LMMSE even when one subsymbol is not allocated. Moreover, with slight performance loss, the diagonal approximation of LMMSE-CEq is dedicated for practical implementation.

Inspired from this model, an efficient GFDMA model is proposed, where the allocation is moved from the data symbol to the FD samples. This model brings additional flexibility to GFDMA, which is a subject of a future work.

References

[1] N. Michailow *et al.*, "Generalized frequency division multiplexing for 5th generation cellular networks," *IEEE Trans. Commun.*, vol. 62, no. 9, pp. 3045–3061, Sep. 2014.

[2] M. Danneberg *et al.*, "Flexible GFDM implementation in FPGA with support to run-time reconfiguration," in *IEEE VTC Fall*, 2015, pp. 1–2.

[3] ——, "Universal waveforms processor," in *IEEE EuCNC*, 2018, pp. 357–362.

[4] S. Tiwari and S. S. Das, "Low-Complexity Joint-MMSE GFDM Receiver," *IEEE Trans. Commun.*, vol. 66, no. 4, pp. 1661–1674, April 2018.

[5] P. Chen *et al.*, "Matrix Characterization for GFDM: Low Complexity MMSE Receivers and Optimal Filters," *IEEE Trans. Signal Process.*, vol. 65, no. 18, pp. 4940–4955, Sept 2017.

[6] M. Matthe *et al.*, "Reduced complexity calculation of LMMSE filter coefficients for GFDM," in *IEEE VTC Fall*, Sept 2015, pp. 1–2.

[7] ——, "Multi-user time-reversal STC-GFDMA for future wireless networks," *EURASIP*, vol. 2015, no. 1, p. 132, 2015.

[8] B. Lim and Y.-C. Ko, "SIR analysis of OFDM and GFDM waveforms with timing offset, CFO, and phase noise," *IEEE Trans. Wireless Commun.*, vol. 16, no. 10, pp. 6979–6990, 2017.

[9] A. Nimr *et al.*, "Optimal radix-2 FFT compatible filters for GFDM," *IEEE Commun. Lett.*, vol. 21, no. 7, pp. 1497–1500, 2017.

[10] I. Gaspar *et al.*, "Low Complexity GFDM Receiver Based on Sparse Frequency Domain Processing," in *IEEE VTC Spring*, 2013, pp. 1–6.

[11] A. Nimr *et al.*, "Unified Low Complexity Radix-2 Architectures for Time and Frequency-domain GFDM Modem," *IEEE CASM*, vol. 18, no. 4, pp. 18–31, 2018.

[12] ——, "Extended GFDM Framework: OTFS and GFDM Comparison," *arXiv preprint arXiv:1808.01161, accepted in IEEE GLOBECOM*, 2018.

[13] M. Matthé *et al.*, "Generalized frequency division multiplexing in a gabor transform setting," *IEEE Commun. Lett.*, vol. 18, no. 8, pp. 1379–1382, 2014.

[14] A. Nimr *et al.*, "A study on the physical layer performance of GFDM for high throughput wireless communication," in *IEEE EUSIPCO*. IEEE, 2017, pp. 638–642.

© 2019 IEEE. Personal use of this material is permitted. Permission from IEEE must be obtained for all other uses, in any current or future media, including reprinting/republishing this material for advertising or promotional purposes, creating new collective works, for resale or redistribution to servers or lists, or reuse of any copyrighted component of this work in other works.